Chaos, Solitons and Fractals 170 (2023) 113361

Contents lists available at ScienceDirect

Chaos, Solitons and Fractals

journal homepage: www.elsevier.com/locate/chaos

Ebola epidemic model with dynamic population and memory

Faïçal Ndaïrou [a,*], Moein Khalighi [b], Leo Lahti [b]

[a] Center for Research and Development in Mathematics and Applications (CIDMA), Department of Mathematics, University of Aveiro, 3810-193 Aveiro, Portugal
[b] Department of Computing, University of Turku, Turku, Finland

ARTICLE INFO

Dataset link: https://doi.org/10.5281/zenodo.7646063

MSC:
34A08
92D30

Keywords:
Ebola model
Basic reproduction ratio
Fractional Ebola model
Fractional derivative
Numerical simulations

ABSTRACT

The recent outbreaks of Ebola encourage researchers to develop mathematical models for simulating the dynamics of Ebola transmission. We continue the study of the models focusing on those with a variable population. Hence, this paper presents a compartmental model consisting of 8-dimensional nonlinear differential equations with a dynamic population and investigates its basic reproduction number. Moreover, a dimensionless model is introduced for numerical analysis, thus proving the disease-free equilibrium is locally asymptotically stable whenever the threshold condition, known as a basic reproduction number, is less than one. Finally, we use a fractional differential form of the model to sufficiently fit long time-series data of Guinea, Liberia, and Sierra Leone retrieved from the World Health Organization, and the numerical results demonstrate the performance of the model.

1. Introduction

Ebola is a highly pernicious virus transmitted by physical contact with body fluids, secretions, tissues, or semen from infected persons. At least 18 confirmed outbreaks of Ebola were recorded in Africa between 1976 and 2014. Up to 2012, about 2400 cases and 1600 deaths were registered due to the Ebola virus. The new outbreak of Ebola started in West Africa on 27th March 2014 and includes 28602 confirmed cases and 11301 deaths.

Recently some compartmental models of Ebola epidemics have been developed [1–6]. Some models in the literature (e.g. [7–9]) have made an attempt to model previous outbreaks of Ebola based on a smaller amount of information as compared to the 2014 outbreak. Several approaches have been presented to model the spread of this disease in the three affected countries in the 2014 outbreak, namely Guinea, Liberia, and Sierra Leone. In [2], the optimal control problem of the Ebola epidemic with vaccination constraints has been considered by introducing an extra variable for the number of vaccines. In some studies, [4,10], the incorporation of fractional derivatives into the models has been introduced. Moreover, in [1] a compartmental model for Ebola consisting of eight nonlinear fractional differential equations (FDE) has been meticulously analyzed.

Here, we continue and improve the mathematical model for the transmission of Ebola proposed in [1]. The main drawback of that model is overlooking the variability of the population as pandemics affected a proportion of the population, additionally, the birth and death rates are quite different in the three mentioned countries. Hence, the novelty of our model is a simulation of the epidemic dynamics of Ebola with a varying population.

The paper is organized as follows. We first introduce the nonlinear system equations under the assumptions of having a varying population N and describe the parameters involved in the system. Next, an equivalent system is presented after introducing an appropriate change of variable. For this equivalent system, the basic reproduction number is explicitly given in terms of the parameters that appear in the differential system. Moreover, a dimensionless compartmental model is introduced. For this dimensionless model, the local stability of the disease-free equilibrium (DFE) point is analyzed. A fractional compartmental model with a varying population is also introduced. Finally, some numerical simulations compared with real data provided by the World Health Organization (WHO) are included.

2. Initial model

Let us suppose that the varying population N is partitioned into eight mutually exclusive compartments: susceptible (S), exposed (E), infected (I), hospitalized (H), asymptomatic but still infectious (R), dead but not buried (L), buried (B), and completely recovered (C) individual classes. The class of completed recovered (C) has been

* Corresponding author.
E-mail addresses: faical@ua.pt (F. Ndaïrou), moein.khalighi@utu.fi (M. Khalighi), leo.lahti@utu.fi (L. Lahti).

https://doi.org/10.1016/j.chaos.2023.113361
Received 11 December 2022; Received in revised form 19 February 2023; Accepted 10 March 2023

Table 1
The parameters of the model described in the system (1).

α_1 :	Density independent part of the birth rate for individuals.
α_2 :	Density dependent part of the birth rate for individuals.
β_i :	Contact rate of infective individuals and susceptible.
β_h :	Contact rate of infective individuals and hospitalized.
β_d :	Contact rate of infective individuals and dead.
β_r :	Contact rate of infective individuals and asymptomatic.
σ :	Per capita rate at which exposed individuals become infectious.
γ_1 :	Per capita rate of progression of individuals from the infectious class to the asymptomatic class.
γ_2 :	Per capita rate of progression of individuals from the hospitalized class to the asymptomatic class.
γ_3 :	Per capita recovery rate of individuals from the asymptomatic class to the complete recovered class.
ϵ :	Fatality rate.
τ :	Per capita rate of progression of individuals from the infectious class to the hospitalized class.
ξ :	incineration rate
δ_1 :	Per capita rate of progression of individuals from the dead class to the buried class.
δ_2 :	Per capita rate of progression of individuals from the hospitalized class to the buried class.
μ_1 :	Density independent part of the death rate for individuals.
μ_2 :	Density dependent part of the death rate for individuals.

already considered in [1] and the evolution of the disease confirms the necessity of considering this class as separated from the recovered class.

Parameters describing the behavior of the dynamics of individuals between these compartments are introduced in Table 1. We assume that the density independent part of the birth rate (α_1) is greater than the density independent part of the death rate (μ_1) which is also greater than the incineration rate (ξ), that is $\alpha_1 > \mu_1$ and $\mu_1 < \xi$. The birth and death terms are assumed to be density dependent on the population size and represented by $\alpha_1 - \alpha_2 N$ and $\mu_1 + \mu_2 N$, respectively, both are strictly monotone continuously differentiable functions with respect to N.

The model is mathematically expressed by the following system of eight nonlinear ordinary differential equations (ODE):

$$\begin{cases} \frac{dS}{dt} = (\alpha_1 - \alpha_2 N)N - \frac{\beta_i}{N} SI - \frac{\beta_h}{N} SH - \frac{\beta_d}{N} SL - \frac{\beta_r}{N} SR - (\mu_1 + \mu_2 N)S, \\ \frac{dE}{dt} = \frac{\beta_i}{N} SI + \frac{\beta_h}{N} SH + \frac{\beta_d}{N} SL + \frac{\beta_r}{N} SR - \sigma E - (\mu_1 + \mu_2 N)E, \\ \frac{dI}{dt} = \sigma E - (\gamma_1 + \epsilon + \tau + \mu_1 + \mu_2 N)I, \\ \frac{dR}{dt} = \gamma_1 I + \gamma_2 H - (\gamma_3 + \mu_1 + \mu_2 N)R, \\ \frac{dL}{dt} = \epsilon I - (\delta_1 + \xi)L, \\ \frac{dH}{dt} = \tau I - (\gamma_2 + \delta_2 + \mu_1 + \mu_2 N)H, \\ \frac{dB}{dt} = \delta_1 L + \delta_2 H - \xi B, \\ \frac{dC}{dt} = \gamma_3 R - (\mu_1 + \mu_2 N)C. \end{cases} \tag{1}$$

Remark 1. The mortality rate of Ebola varies from 50% to 90%. Very recently a new study provided strong evidence that individual genetic differences play a major role in whether people die from the disease [11]. In the 2014 outbreak, the mean incubation period is 11.4 days and does not vary by country [12]. The mean time from the onset of symptoms to hospitalization, a measure of the period of infectiousness in the community, is 5.0 ± 4.7 days, and it is not shorter for healthcare workers than for other case patients. The mean time to death after admission to the hospital is 4.2 ± 6.4 days, and the mean time to discharge is 11.8 ± 6.1 days [12] .

The population size is $N(t) = S(t) + E(t) + I(t) + R(t) + L(t) + H(t) + B(t) + C(t)$. By adding up all the eight equations we have

$$\frac{dN}{dt}(t) = (\alpha_2 + \mu_2)N^2(t) + (\alpha_1 - \mu_1)N(t) - (\xi - \mu_1 - \mu_2 N(t))(L(t) + B(t)).$$

Next, by substituting S by $N-E-I-R-L-H-B-C$, we can transform (1) into the following system which is practical for the analysis

$$\begin{cases} \frac{dE}{dt} = \frac{1}{N}(\beta_i I + \beta_h H + \beta_d L + \beta_r R)(N - E - I - R - L - H - B - C) \\ \qquad\qquad -\sigma E - (\mu_1 + \mu_2 N)E, \\ \frac{dI}{dt} = \sigma E - (\gamma_1 + \epsilon + \tau + \mu_1 + \mu_2 N)I, \\ \frac{dR}{dt} = \gamma_1 I + \gamma_2 H - (\gamma_3 + \mu_1 + \mu_2 N)R, \\ \frac{dL}{dt} = \epsilon I - (\delta_1 + \xi)L, \\ \frac{dH}{dt} = \tau I - (\gamma_2 + \delta_2 + \mu_1 + \mu_2 N)H, \\ \frac{dB}{dt} = \delta_1 L + \delta_2 H - \xi B, \\ \frac{dC}{dt} = \gamma_3 R - (\mu_1 + \mu_2 N)C, \\ \frac{dN}{dt} = -(\alpha_2 + \mu_2)N^2 + (\alpha_1 - \mu_1)N - (\xi - \mu_1 - \mu_2 N)(L + B). \end{cases} \tag{2}$$

Following the same approach as in [1], we can determine the basic reproduction number for model (2) as

$$R_0 = \frac{\sigma\left(\beta_i a_1 a_2 a_3 + a_3(a_1\gamma_1 + \tau\gamma_2)\beta_r + a_1 a_2 \epsilon \beta_d + a_2 a_3 \tau \beta_h\right)}{a_1 a_2 a_3 \left(\gamma_1 + \epsilon + \tau + a_5\right)\left(\sigma + a_5\right)},$$

with

$$a_1 = \gamma_2 + \delta_2 + \mu_1 + \mu_2 N^*, \quad a_2 = \gamma_3 + \mu_1 + \mu_2 N^*, \quad a_3 = \delta_1 + \xi, \quad a_4 = \gamma_2 + \delta_2,$$
$$a_5 = \mu_1 + \mu_2 N^*, \quad \text{and} \quad N^* = \frac{\alpha_1 - \mu_1}{\alpha_2 + \mu_2}$$

As it is well known, if $R_0 < 1$ then each infected individual produces less than one new infected individual, and the infection cannot spread. On the other hand, if $R_0 > 1$, then on average of infected individual yields more than one infected individual, and as a result of that, the disease can spread in the population.

3. Dimensionless compartmental model of Ebola

In order to simplify the analysis of the Ebola model (2), the following scaled variables are used

$$e = \frac{E}{e^0}, \ i = \frac{I}{i^0}, \ r = \frac{R}{r^0}, \ l = \frac{L}{l^0}, \ h = \frac{H}{h^0}, \ c = \frac{C}{c^0}, \ n = \frac{N}{n^0}, \ \text{and} \ \theta = \frac{t}{T^0},$$

where $e^0, i^0, r^0, l^0, h^0, c^0$ and T^0, s^0 are some reference positive variables to be determined. By substituting the scaled populations e, i, r, l, h,

c and n in the model (2) as well as θ, we can obtain the following parameterized system

$$\begin{cases}
\frac{de}{d\theta} = (T^0\beta_i i^0 i + T^0\beta_h h^0 h + T^0\beta_d l^0 l + T^0\beta_r r^0 r)\left(\frac{1}{e^0} - \frac{e}{n^0 n} - \frac{i^0 i}{n^0 n e^0} - \frac{r^0 r}{n^0 n e^0} - \frac{l^0 l}{n^0 n e^0} - \frac{h^0 h}{n^0 n e^0} - \frac{b^0 b}{n^0 n e^0} - \frac{c^0 c}{n^0 n e^0}\right) - T^0(\sigma+\mu_1)e - T^0\mu_2 n^0 n e,\\
\frac{di}{d\theta} = \frac{T^0 e^0}{i^0}\sigma e - T^0(\gamma_1+\epsilon+\tau+\mu_1)i - T^0\mu_2 n^0 n i,\\
\frac{dr}{d\theta} = \frac{T^0 i^0}{r^0}\gamma_1 i + \frac{T^0 h^0}{r^0}\gamma_2 h - T^0(\gamma_3+\mu_1)r - T^0\mu_2 n^0 n r,\\
\frac{dl}{d\theta} = \frac{T^0 i^0}{l^0}\epsilon i - T^0(\delta_1+\xi)l,\\
\frac{dh}{d\theta} = \frac{T^0 i^0}{h^0}\tau i - T^0(\gamma_2+\delta_2+\mu_1)h - T^0\mu_2 n^0 n h,\\
\frac{db}{d\theta} = \frac{T^0\delta_1 l^0}{b^0}l + \frac{T^0\delta_2 h^0}{b^0}h - T^0\xi b,\\
\frac{dc}{d\theta} = \frac{T^0 r^0}{c^0}\gamma_3 r - T^0\mu_1 c - T^0\mu_2 n^0 n c,\\
\frac{dn}{d\theta} = -T^0(\alpha_2+\mu_2)n^0 n^2 + T^0(\alpha_1-\mu_1)n - T^0(\xi-\mu_1)\frac{l^0 l + b^0 b}{n^0} + T^0\mu_2(l^0 l + b^0 b)n.
\end{cases} \tag{3}$$

Let us consider

$$T^0 = \frac{1}{\alpha_1-\mu_1},\quad n^0 = \frac{1}{T^0(\alpha_2+\mu_2)},\quad e^0 = \frac{n^0}{T^0},\quad i^0 = T^0\sigma e^0,\quad r^0 = T^0\gamma_1 i^0$$
$$l^0 = T^0\epsilon i^0,\quad h^0 = T^0\tau i^0,\quad b^0 = T^0 l^0\delta_1,\quad c^0 = T^0 r^0\gamma_3.$$

Next, we define the parameter grouping as

$$A_1 = T^0\beta_i i^0,\quad A_2 = T^0\beta_h h^0,\quad A_3 = T^0\beta_d l^0,\quad A_4 = T^0\beta_r r^0,$$
$$A_5 = \frac{1}{e^0},\quad A_6 = \frac{1}{n^0},$$
$$A_7 = \frac{i^0}{n^0 e^0},\quad A_8 = \frac{r^0}{n^0 e^0},\quad A_9 = \frac{l^0}{n^0 e^0},\quad A_{10} = \frac{h^0}{n^0 e^0},$$
$$A_{11} = \frac{b^0}{n^0 e^0},\quad A_{12} = \frac{c^0}{n^0 e^0},$$
$$A_{13} = T^0(\sigma+\mu_1),\quad A_{14} = T^0\mu_2 n^0,$$
$$A_{15} = T^0(\gamma_1+\epsilon+\tau+\mu_1),\quad A_{16} = T^0(\gamma_3+\mu_1),$$
$$A_{17} = \frac{T^0 h^0}{r^0}\gamma_2,\quad A_{18} = T^0(\delta_1+\xi),$$
$$A_{19} = T^0(\gamma_2+\delta_2+\mu_1),\quad A_{20} = \frac{T^0\delta_2 h^0}{b^0},$$
$$A_{21} = T^0\xi,\quad A_{22} = T^0\mu_1,\quad A_{23} = \frac{T^0 b^0(\mu_1-\xi)}{n^0},\quad A_{24} = \frac{T^0 l^0(\mu_1-\xi)}{n^0},$$
$$A_{25} = T^0\mu_2 l^0,\quad A_{26} = T^0\mu_2 b^0.$$

Therefore from (3) we obtain the following dimensionless system equivalent to (1)

$$\begin{cases}
\frac{de(\theta)}{d\theta} = (A_1 i(\theta) + A_2 h(\theta) + A_3 l(\theta) + A_4 r(\theta))\left(A_5 - \frac{A_6 e(\theta)}{n(\theta)} - \frac{A_7 i(\theta)}{n(\theta)} - \frac{A_8 r(\theta)}{n(\theta)} - \frac{A_9 l(\theta)}{n(\theta)} - \frac{A_{10} h(\theta)}{n(\theta)} - \frac{A_{11} b(\theta)}{n(\theta)} - \frac{A_{11} c(\theta)}{n(\theta)}\right) - A_{13} e(\theta) - A_{14} n(\theta) e(\theta),\\
\frac{di(\theta)}{d\theta} = e(\theta) - A_{15} i(\theta) - A_{14} n(\theta) i(\theta),\\
\frac{dr(\theta)}{d\theta} = i(\theta) - A_{16} r(\theta) + A_{17} h(\theta) - A_{14} n(\theta) r(\theta),\\
\frac{dl(\theta)}{d\theta} = i(\theta) - A_{18} l(\theta),\\
\frac{dh(\theta)}{d\theta} = i(\theta) - A_{19} h(\theta) - A_{14} n(\theta) h(\theta),\\
\frac{db(\theta)}{d\theta} = l(\theta) + A_{20} h(\theta) - A_{21} b(\theta),\\
\frac{dc(\theta)}{d\theta} = r(\theta) - A_{22} c(\theta) - A_{14} n(\theta) c(\theta),\\
\frac{dn(\theta)}{d\theta} = -n^2(\theta) + n(\theta) + A_{25} n(\theta) b(\theta) + A_{26} n(\theta) l(\theta) + A_{24} l(\theta) + A_{23} b(\theta).
\end{cases} \tag{4}$$

3.1. Local stability of the disease-free equilibrium

The Jacobian matrix of the system (4) at $DFE = (0,0,0,0,0,0,0,1)$ is the 8×8 matrix given in Box I.

By removing the two last columns and rows, we obtain the following 6×6 matrix

$$\tilde{J} = \begin{pmatrix}
-A_{13}-A_{14} & A_1A_5 & A_4A_5 & A_3A_5 & A_2A_5 & 0\\
1 & -A_{15}-A_{14} & 0 & 0 & 0 & 0\\
0 & 1 & -A_{16}-A_{14} & 0 & A_{17} & 0\\
0 & 1 & 0 & -A_{18} & 0 & 0\\
0 & 1 & 0 & 0 & -A_{19}-A_{14} & 0\\
0 & 0 & 0 & 1 & A_{20} & -A_{21}
\end{pmatrix}.$$

Again, as the last column has negative diagonal entries, we can remove it and its corresponding row to obtain

$$\bar{J} = \begin{pmatrix}
-A_{13}-A_{14} & A_1A_5 & A_4A_5 & A_3A_5 & A_2A_5\\
1 & -A_{15}-A_{14} & 0 & 0 & 0\\
0 & 1 & -A_{16}-A_{14} & 0 & A_{17}\\
0 & 1 & 0 & -A_{18} & 0\\
0 & 1 & 0 & 0 & -A_{19}-A_{14}
\end{pmatrix}. \tag{5}$$

The eigenvalues of the (5×5)-matrix $\bar{J}$ are the roots of the characteristic polynomial

$$P(\lambda) = \lambda^5 + x_1\lambda^4 + x_2\lambda^3 + x_3\lambda^2 + x_4\lambda + x_5, \tag{6}$$

where

$$\begin{aligned}
x_1 &= A_{19} + 4A_{14} + A_{13} + A_{16} + A_{15} + A_{18},\\
x_2 &= (2A_{14} + A_{16} + A_{18} + A_{19})(A_{13} + A_{15})\\
&\quad + (4A_{18} + 5A_{14} + 3A_{19} + 3A_{16})A_{14}\\
&\quad + A_{16}(A_{18} + A_{19}) + A_{18}A_{19} + \varpi_1 - A_1A_5,\\
x_3 &= (A_{13} + 2A_{14} + A_{15})[A_{14}(A_{16} + A_{19} + 2A_{18} + A_{14})\\
&\quad + A_{16}(A_{18} + A_{19}) + A_{18}A_{19}]\\
&\quad + A_{14}A_{18}(A_{16} + A_{19} + A_{14}) + A_{16}A_{18}A_{19} + A_{18}\varpi_1 - A_5(A_3 + A_1A_{18})\\
&\quad + \varpi_2 - A_5[A_2 + A_1(A_{14} + A_{19})] + \varpi_3 - A_5[A_4 + A_1(A_{14} + A_{16})],\\
x_4 &= A_{18}(A_{13} + 2A_{14} + A_{15})[A_{14}(A_{14} + A_{16} + A_{19})\\
&\quad + A_{16}A_{19}] + A_{18}\varpi_2 - A_5[A_2A_{18}\\
&\quad + (A_1A_{18} + A_3)(A_{14} + A_{19})] + A_{18}\varpi_3\\
&\quad - A_5[(A_1A_{18} + A_3)(A_{14} + A_{16}) + A_4A_{18}]\\
&\quad + \varpi_4 - A_5[A_1(A_{14} + A_{19})(A_{14} + A_{16})\\
&\quad + A_4(A_{19} + A_{14} + A_{17}) + A_2(A_{16} + A_{14})],\\
x_5 &= A_{18}\varpi_4 - A_5\varpi_5,
\end{aligned}$$

with

$$\begin{aligned}
\varpi_1 &= (A_{14} + A_{15})(A_{13} + A_{14}),\\
\varpi_2 &= (A_{14} + A_{19})(A_{14} + A_{15})(A_{13} + A_{14}),\\
\varpi_3 &= (A_{14} + A_{16})(A_{14} + A_{15})(A_{13} + A_{14}),\\
\varpi_4 &= (A_{14} + A_{16})(A_{14} + A_{19})(A_{14} + A_{15})(A_{13} + A_{14}),\\
\varpi_5 &= (A_{14} + A_{16})(A_{14} + A_{19})(A_1A_{18} + A_3) + A_4A_{18}(A_{19} + A_{14} + A_{17})\\
&\quad + A_2A_{18}(A_{16} + A_{14}).
\end{aligned}$$

By using Liénard–Chipart test [13,14], all the roots of $P(\lambda)$ are negative or have negative real part if and only if the following conditions are satisfied:

1. $x_i > 0, i = 1,2,3,4,5,$
2. $x_1x_2x_3 > x_3^2 + x_1^2x_4.$

Let us introduce the basic reproduction number

$$R_0 = \frac{A_5\times\varpi_5}{A_{18}\times\varpi_4} \tag{7}$$

$$J = \begin{pmatrix} -A_{13}-A_{14} & A_1A_5 & A_4A_5 & A_3A_5 & A_2A_5 & 0 & 0 & 0 \\ 1 & -A_{15}-A_{14} & 0 & 0 & 0 & 0 & 0 & 0 \\ 0 & 1 & -A_{16}-A_{14} & 0 & A_{17} & 0 & 0 & 0 \\ 0 & 1 & 0 & -A_{18} & 0 & 0 & 0 & 0 \\ 0 & 1 & 0 & 0 & -A_{19}-A_{14} & 0 & 0 & 0 \\ 0 & 0 & 0 & 1 & A_{20} & -A_{21} & 0 & 0 \\ 0 & 0 & 1 & 0 & 0 & 0 & -A_{22}-A_{14} & 0 \\ 0 & 0 & 0 & A_{26}-A_{24} & 0 & A_{25}-A_{23} & 0 & -1 \end{pmatrix}.$$

Box I.

obtained using the next generation matrix [15]. The coefficients $x_1, \ldots, x_5$ of the characteristic polynomial $P(\lambda)$ defined in (6) can be rewritten in terms of the basic reproduction number R_0 as:

$$\begin{aligned}
x_1 &= A_{19} + 4A_{14} + A_{13} + A_{16} + A_{15} + A_{18},\\
x_2 &= (2A_{14} + A_{16} + A_{18} + A_{19})(A_{13} + A_{15})\\
&\quad + (4A_{18} + 5A_{14} + 3A_{19} + 3A_{16})A_{14} + A_{16}A_{18}\\
&\quad + A_{16}A_{19} + A_{18}A_{19} + (1-R_0)\varpi_1 + \frac{A_3A_5}{A_{18}}\\
&\quad + \frac{A_2A_5}{A_{19}+A_{14}} + \frac{(A_{19}+A_{14}+A_{17})\,A_4A_5}{(A_{16}+A_{14})\,(A_{19}+A_{14})},\\
x_3 &= (A_{13}+2A_{14}+A_{15})[A_{14}(A_{16}+A_{19}+2A_{18}+A_{14})\\
&\quad + A_{16}(A_{18}+A_{19}) + A_{18}A_{19}]\\
&\quad + A_{14}A_{18}(A_{16}+A_{19}+A_{14}) + A_{16}A_{18}A_{19} + (1-R_0)(\varpi_3 + \varpi_2 + A_{18}\varpi_1)\\
&\quad + \frac{A_3A_5\,(2A_{14}+A_{16}+A_{19})}{A_{18}} + \frac{(A_2A_{14}+A_2A_{18}+A_2A_{16}+A_4A_{17})\,A_5}{A_{19}+A_{14}}\\
&\quad + \frac{A_4\,(A_{19}+A_{18}+A_{14})\,(A_{19}+A_{14}+A_{17})\,A_5}{(A_{16}+A_{14})\,(A_{19}+A_{14})},\\
x_4 &= A_{18}(A_{13}+2A_{14}+A_{15})[A_{14}(A_{14}+A_{16}+A_{19}) + A_{16}A_{19}]\\
&\quad + (1-R_0)(\varpi_4 + (\varpi_3+\varpi_2)A_{18})\\
&\quad + \frac{A_3A_5\,(A_{16}+A_{14})\,(A_{19}+A_{14})}{A_{18}} + \frac{(A_2A_{14}+A_2A_{16}+A_4A_{17})\,A_{18}A_5}{A_{19}+A_{14}}\\
&\quad + \frac{A_4A_{18}\,(A_{19}+A_{14}+A_{17})\,A_5}{A_{16}+A_{14}},\\
x_5 &= A_{18}\varpi_4(1-R_0).
\end{aligned}$$

From the above expressions, it is easy to check that the first conditions of the Liénard–Chipart test ($x_i > 0$) are satisfied when $R_0 < 1$. In the case $R_0 > 1$ we have that $x_5 < 0$ and by using Descartes' rule of signs we have that at least one eigenvalue is positive and therefore the system is unstable.

Moreover, in order to check the second condition of the Liénard–Chipart test, after some computations we have expressed $x_1x_2x_3 - (x_3^2 + x_1^2x_4)$ in terms of $1-R_0$. In this form we have obtained that all the terms in the latter expression are positive except the following one involving some negative terms

$$\begin{aligned}
Y &= (A_{14}+A_{15})\,(A_{13}+A_{14})\,A_{18}\,(A_{14}+A_{19})\,(A_{14}+A_{16})\,\Big(\,24\,{A_{14}}^4\\
&+{A_{16}}^2A_{18}A_{15} + {A_{18}}^2A_{15}A_{16} + {A_{18}}^2A_{15}A_{19} + 2\,{A_{13}}^2A_{18}A_{16}\\
&+2\,{A_{13}}^2A_{18}A_{19} + 2\,A_{18}{A_{15}}^2A_{16} + 2\,A_{18}{A_{15}}^2A_{19} + {A_{18}}^2A_{13}A_{16}\\
&+{A_{18}}^2A_{13}A_{19} - A_{18}{A_{16}}^2A_{19} - A_{18}{A_{19}}^2A_{16} + 2\,{A_{18}}^2A_{15}A_{13} + {A_{16}}^2A_{18}A_{13}\\
&+4\,A_{15}A_{19}A_{13}A_{16} + 11\,A_{14}A_{18}A_{15}A_{16} + 12\,A_{14}A_{19}A_{16}A_{15}\\
&+12\,A_{14}A_{19}A_{16}A_{13} + 11\,A_{14}A_{18}A_{13}A_{16} + 11\,A_{14}A_{18}A_{19}A_{13}\\
&+8\,A_{14}A_{16}A_{13}A_{15} + 8\,A_{14}A_{19}A_{13}A_{15} + 8\,A_{14}A_{18}A_{13}A_{15}\\
&+11\,A_{14}A_{18}A_{19}A_{15} - 2\,A_{18}A_{19}A_{16}A_{14} + A_{18}{A_{19}}^2A_{14} + 16\,A_{19}{A_{14}}^2A_{16}\\
&+2\,A_{15}{A_{16}}^2A_{13} + 2\,A_{15}{A_{19}}^2A_{13} + 2\,A_{19}{A_{15}}^2A_{16} + 2\,A_{19}{A_{13}}^2A_{16}\\
&+A_{19}A_{13}{A_{16}}^2 + A_{19}A_{15}{A_{16}}^2 + {A_{19}}^2A_{13}A_{16} + {A_{19}}^2A_{15}A_{16}\\
&+19\,{A_{14}}^2A_{18}A_{13} + 22\,{A_{14}}^2A_{16}A_{13} + 22\,{A_{14}}^2A_{19}A_{15} + 22\,{A_{14}}^2A_{19}A_{13}\\
&+8\,{A_{14}}^2A_{15}A_{13} + 19\,{A_{14}}^2A_{18}A_{15} + 22\,{A_{14}}^2A_{16}A_{15} + 8\,A_{14}A_{13}{A_{16}}^2\\
&+8\,A_{14}{A_{19}}^2A_{13} + 4\,A_{14}A_{18}{A_{13}}^2 + 4\,A_{14}A_{18}{A_{15}}^2 + 6\,A_{14}{A_{18}}^2A_{13}\\
&+6\,A_{14}{A_{18}}^2A_{15} + 4\,A_{14}A_{16}{A_{13}}^2 + 4\,A_{14}A_{16}{A_{15}}^2 + 4\,A_{14}A_{19}{A_{13}}^2\\
&+4\,A_{14}A_{19}{A_{15}}^2 + 8\,A_{14}{A_{16}}^2A_{15} + 8\,A_{14}{A_{19}}^2A_{15} + 2\,{A_{16}}^2A_{19}A_{14}\\
&+2\,{A_{19}}^2A_{16}A_{14} + A_{18}A_{14}{A_{16}}^2 + {A_{18}}^2A_{14}A_{16} + {A_{18}}^2A_{14}A_{19}\\
&+11\,A_{18}{A_{14}}^2A_{16} + 11\,A_{18}A_{19}{A_{14}}^2 + 2\,{A_{19}}^3A_{14} + 7\,{A_{18}}^2{A_{14}}^2 + 20\,A_{18}{A_{14}}^3\\
&+2\,A_{14}{A_{16}}^3 + 12\,{A_{16}}^2{A_{14}}^2 + 28\,A_{19}{A_{14}}^3 + {A_{19}}^3A_{15} + {A_{15}}^2{A_{16}}^2 + {A_{19}}^2{A_{15}}^2\\
&+{A_{16}}^3A_{13} + {A_{19}}^3A_{13} + {A_{16}}^2{A_{13}}^2 + {A_{19}}^2{A_{13}}^2 + 20\,{A_{14}}^3A_{15} + 20\,{A_{14}}^3A_{13}\\
&+4\,{A_{14}}^2{A_{15}}^2 + 4\,{A_{14}}^2{A_{13}}^2 + 2\,A_{14}{A_{18}}^3 + {A_{16}}^3A_{15} + A_{18}A_{13}A_{19}A_{16}\\
&+A_{18}A_{15}A_{19}A_{16} - A_{16}{A_{18}}^2A_{19} + A_{18}A_{13}{A_{19}}^2 + A_{18}A_{15}{A_{19}}^2\\
&+4\,A_{18}A_{16}A_{15}A_{13} + 12\,{A_{19}}^2{A_{14}}^2 + 28\,A_{16}{A_{14}}^3 + 4\,A_{18}A_{19}A_{15}A_{13}\\
&+{A_{18}}^3A_{15} + {A_{13}}^2{A_{18}}^2 + {A_{18}}^2{A_{15}}^2 + {A_{18}}^3A_{13}\,\Big)
\end{aligned}$$

up to a multiplicative positive constant. It is easy to prove that any of the three following conditions is sufficient to ensure the positivity of Y

$$\begin{aligned}
&A_{13} + A_{15} - 2A_{14} - A_{16} > 0, \text{ or } A_{13} + A_{15} - 2A_{14} - A_{18} > 0,\\
&\text{or } A_{13} + A_{15} - 2A_{14} - A_{19} > 0.
\end{aligned}$$

Hence, any of the latter conditions imply the positivity of $x_1x_2x_3 - (x_3^2 + x_1^2x_4)$, which remained to be proved in order to ensure the sign of the eigenvalues of the Jacobian matrix of the system (4) at $DFE = (0,0,0,0,0,0,0,N^*)$ are all negative. We need to explain that one of the conditions is realistic.

Let us examine the condition $A_{13} + A_{15} - 2A_{14} - A16 > 0$, that is

$$\mu_1 + \sigma + \epsilon + \tau + \gamma_1 - 2\mu_2N^* - \gamma_3 > 0.$$

We notice that it is sufficient to fulfill the following conditions

$$\begin{cases} 2\mu_2N^* < \mu_1 \\ \gamma_3 < \sigma + \epsilon + \tau + \gamma_1 \end{cases}$$

Let us recall that from [1] it has been studied a similar model with constant population and the condition $\frac{\gamma_3+\mu}{\epsilon+\tau+\gamma_1+\mu} < 1$ has been given as realistic. Writing this condition as $\gamma_3 < \epsilon + \tau + \gamma_1$ we can obtain as consequence that $\gamma_3 < \sigma + \epsilon + \tau + \gamma_1$.

Moreover, the condition $2\mu_2N^* < \mu_1$, which is $\frac{\alpha_1-\mu_1}{\alpha_2+\mu_2} < \frac{\mu_1}{2\mu_2}$ can be reduce to satisfy $\alpha_1 < 2\mu_1$ and $\alpha_2 \geq \mu_2$, meaning that to maintain the birth rate less than twice the death rate and the density dependent part of the birth rate greater than the density dependent part of the death rate.

In conclusion, the DFE point is stable if the birth rate is less than twice the death rate and the density dependent part of the birth rate greater than the density dependent part of the death rate. In this case, the basic reproduction number is less than one ($R_0 < 1$).

Remark 2. For a constant population, $\mu_1 = \alpha_1$, $\mu_2 = \alpha_2 = 0$, the above conditions become $\gamma_3 < \sigma + \epsilon + \tau + \gamma_1$ and it is sufficient to consider the condition $\gamma_3 < \epsilon + \tau + \gamma_1$ given in [1].

4. Fractional compartmental model of Ebola

As it has been shown in the literature, one possible physical meaning of non-integer orders in fractional derivatives is as an index of memory [16]. Memory effects can arise in epidemiological models from various sources including individual and population-level changes in the level of immunity, and protective measures [17]. We do not intend to present a review of the main results on fractional calculus, but to introduce the basic definition necessary to present a fractional analog of the system (4).

The Caputo fractional derivative [18,19] of order $\alpha \in (0,1]$ of a function $f : [t_0, +\infty) \to \mathbb{R}$ is given by

$$ {}^{C}D^{\alpha} f(t) = I^{1-\alpha} D^{1} f(t) = \frac{1}{\Gamma(1-\alpha)} \int_{t_0}^{t} (t-s)^{-\alpha} f'(s) ds, $$

which is well defined, for example, for absolutely continuous functions. Note that the value of the Caputo fractional derivative of the function f at point t involves all the values of $f'(s)$ for $s \in [t_0, t]$, and hence it incorporates the history of f. Notice that ${}^{C}D^{\alpha} f(t)$ tends to $f'(t)$ as $\alpha \to 1$.

We write the system (1) in terms of fractional differential equations as

$$ \begin{cases} {}^{C}D^{\alpha_S} S(t) = (\alpha_1 - \alpha_2 N)N - \frac{\beta_i}{N} SI - \frac{\beta_h}{N} SH - \frac{\beta_d}{N} SL \\ \qquad - \frac{\beta_r}{N} SR - (\mu_1 + \mu_2 N)S, \\ {}^{C}D^{\alpha_E} E(t) = \frac{\beta_i}{N} SI + \frac{\beta_h}{N} SH + \frac{\beta_d}{N} SL + \frac{\beta_r}{N} SR - \sigma E - (\mu_1 + \mu_2 N)E, \\ {}^{C}D^{\alpha_I} I(t) = \sigma E - (\gamma_1 + \epsilon + \tau + \mu_1 + \mu_2 N)I, \\ {}^{C}D^{\alpha_R} R(t) = \gamma_1 I + \gamma_2 H - (\gamma_3 + \mu_1 + \mu_2 N)R, \\ {}^{C}D^{\alpha_L} L(t) = \epsilon I - (\delta_1 + \xi)L, \\ {}^{C}D^{\alpha_H} H(t) = \tau I - (\gamma_2 + \delta_2 + \mu_1 + \mu_2 N)H, \\ {}^{C}D^{\alpha_B} B(t) = \delta_1 L + \delta_2 H - \xi B, \\ {}^{C}D^{\alpha_C} C(t) = \gamma_3 R - (\mu_1 + \mu_2 N)C. \end{cases} \tag{8} $$

This system includes incommensurate order derivatives, $\alpha_{i=S,E,I,R,L,H,B,C}$, which means the orders could be unequal.

5. Numerical results

In this section, we present the effectiveness of our proposed model, which incorporates a variable population, in fitting real-world data acquired from the World Health Organization. The estimation of infectious disease model parameters is a challenging task due to the difficulty in determining the initial value of susceptible individuals. Moreover, the assumption of a standard incidence rate, which implies that the ratio of susceptible individuals to the total population is approximately 1, is only valid when the total population remains constant. In situations where the total population N is varying, the carrying capacity of the system is an asymptotic value, making it more challenging to determine the initial conditions for the varying aspects of population dynamics. Given these challenges and taking note of previous studies [1,2], which utilized and considered initial conditions of 18000, 24500, and 23700 for susceptible individuals, we assume in our analysis a minimum initial value of $S_0 = 18000$, with the understanding that other values can be achieved through the evolution of the system's dynamics. Hence, the initial conditions for our model are as follows:

$$ \begin{aligned} &S_0 = 18000,\ E_0 = 0,\ I_0 = 15,\ R_0 = 0,\ L_0 = 0,\ H_0 = 0,\ B_0 = 0,\ C_0 = 0, \\ &N_0 = S_0 + E_0 + I_0 + R_0 + L_0 + H_0 + B_0 + C_0, \end{aligned} \tag{9} $$

and values of parameters from Ref. [1,2]:

$$ \begin{cases} \alpha_1 = 0.03537, \quad \sigma = 1/11.4, \quad \epsilon = 1/9.6, \quad \delta_1 = 0.5, \\ \delta_2 = 1/4.6, \quad \tau = 0.2, \quad \beta_i = 0.14, \quad \beta_d = 0.40, \quad \xi = 14\text{e}{-3} \\ \beta_h = 0.29, \quad \mu_1 = 1.017\text{e}{-4}, \quad \gamma_1 = 1/10, \quad \gamma_2 = 1/5, \quad \gamma_3 = 1/30. \end{cases} \tag{10} $$

We compare the efficiency of the four models described in the following for the simulation of real data.

- **Model 1**: The original model from Ref. [2] with considering constant population N and death rate $\mu = \mu_1 + \mu_2 N$ and birth rate $\mu = \alpha_1 - \alpha_2 N$.
- **Model 2**: The ODE model (1), with integer orders.
- **Model 3**: The FDE model (8), with incommensurate fractional orders from the initial time (day 4).
- **Model 4**: The ODE model (1) from the initial time (day 4) to a day after 216 and continuing with the incommensurate FDE model (8) to the final time (day 438).

The data is provided for the cumulative confirmed cases from day 4 to 438 including a sudden jump within days 212–216, from 5666 to 7606. This jump affects the fitting. Thus, Model 4 suggests a piecewise differential equation such that its dynamics are initially memoryless but after the jump incorporates memory effects. We approximate the values of β_r and μ for Model 1. We need to estimate β_r together with the new parameters α_2 and μ_2 for Model 2, and optimize the values of order derivatives for Model 3 and 4 when using the fitted parameters from Model 2. Table 2 shows the fitted values and their root mean square deviation (RMSD) for all models, such that $\text{RMSD}(x, \hat{x}) = \sqrt{\frac{1}{n}\sum_{t=1}^{n}(x_t - \hat{x}_t)^2}$, where, n is the number of data points, x approximated values, and $\hat{x}$ real values.

Fig. 1 (a) illustrates how the models fit the data. Model 1, which had a constant population, is not flexible enough to fit the data well, resulting in a high error of 2085. Model 2, which replaced parameter μ with four new parameters, $\alpha_1, \alpha_2, \mu_1$, and μ_2, performs better and improves the simulation to an RMSD error of 276.5. However, the order derivatives of the model need to be adjusted further to fit the last data points more accurately. In Model 3, the fitted order derivatives lead to a slight improvement, with an RMSD error of 245.9. However, the simulation continues to diverge from the data points after day 400, and the result is not monotonically increasing. Model 4 solved this issue and provided the best fit among the models, with an RMSD error of 170.9.

The population dynamics for the models are shown in Fig. 1 (b). Model 1 assumes a constant population size of $N = 18015$, whereas, in other models, the population size is variable and evaluated over the entire time range. In Model 4, the selection of the initial time for utilizing the FDE model is crucial. To determine the optimal fit of the model, we have explored various initial times ranging from day 216 to 300. Our findings indicate that day 280 serves as the most appropriate initial day for using the FDE model, resulting in the least error, as illustrated in Fig. 1 (c). Therefore, we have chosen day 280 as the initial time for applying the FDE model in our analysis. In Fig. 1 (d), we show how Model 4 behaves when altering the derivative order of variable E within the range of $(0.4, 0.98)$. Here, the light blue curve is the dynamics of Model 1 and the dark blue region is the dynamics of Model 4 when $0.4 \leq \alpha_E \leq 0.98$ and other orders are integer one. Fig. 1 (e) is a heatmap of $log10$ of RMSD for Model 3 when the order derivative of each variable (individual classes) is changed from 0.6 to 1. Colors show the RMSD of Model 3 versus order. Orange indicates a

Table 2
The fitted parameters of the studied models with their RMSD errors.

Model 1	$\beta_r = 0.726500,\ \mu = 0.069182$	RMSD=2085
Model 2	$\beta_r = 0.217485,\ \alpha_2 = 8.33457\text{e}{-8},\ \mu_2 = 4.85996\text{e}{-7}$	RMSD=278.5
Model 3	$\alpha_{[S,E,I,R,L,H,B,C]} = [0.94149, 1, 1, 1, 1, 1, 0.94302, 0.79323]$	RMSD=245.9
Model 4	$\alpha_{[S,E,I,R,L,H,B,C]} = [0.5, 0.67349, 0.55635, 0.67598, 0.5, 0.55029, 0.88395, 0.5]$	RMSD=170.9

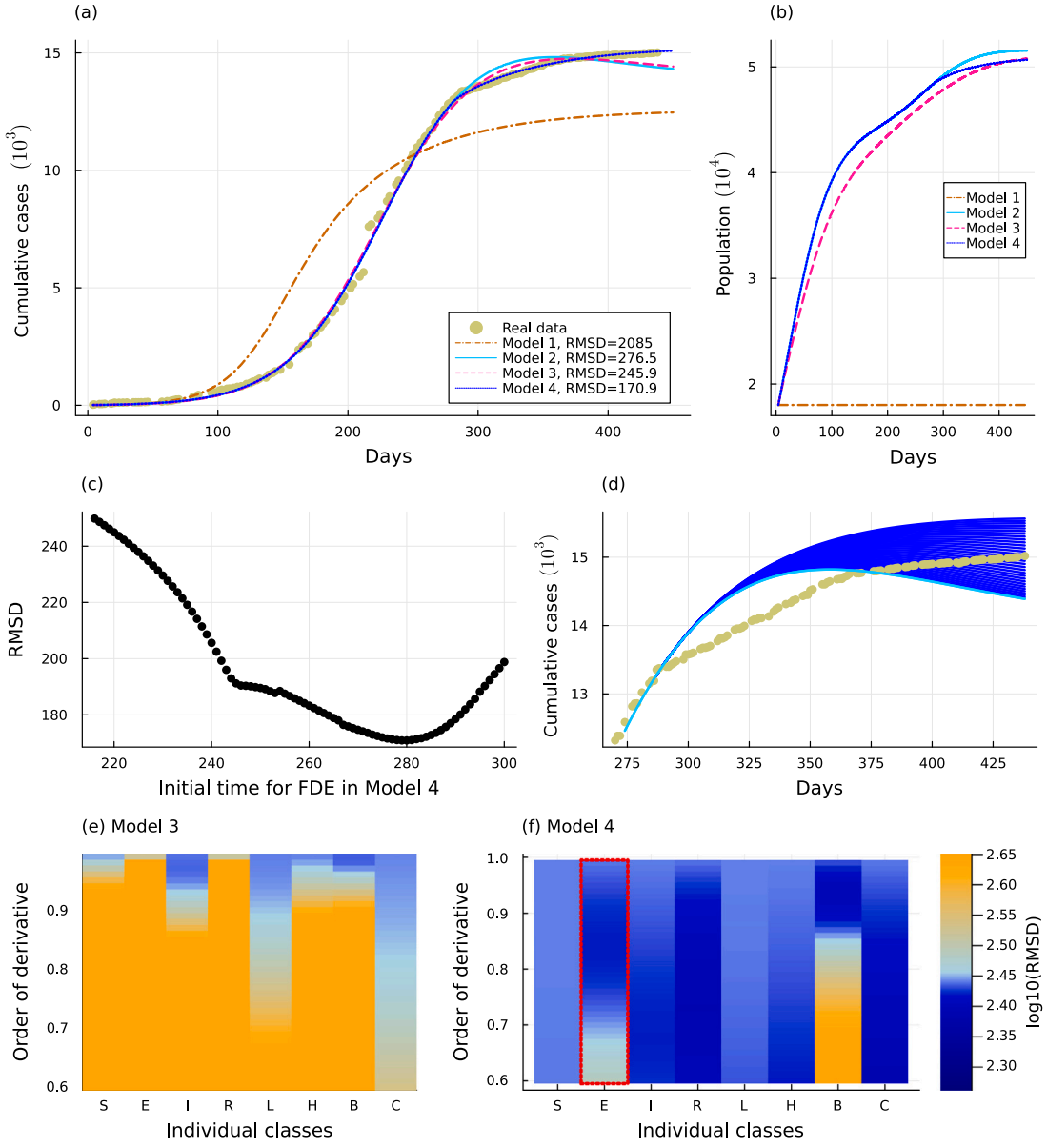

Fig. 1. (a) Fitting the real data with the models. The circles are the time-series data points of cumulative confirmed cases retrieved from WHO for days 4–438. The orange dash–dotted line is the dynamics of $I + R + L + H + B + C - \mu(N - S - E)$ evaluated from Model 1, the model with constant N. The light blue solid line is the dynamics of $I + R + L + H + B + C - \mu_3(N - S - E)$, where $\mu_3 = (\mu_1 + \alpha_1 + (\mu_2 - \alpha_2)N)/2$, evaluated from Model 2. The pink dash line and the dark blue dotted line are the fitted results to the data by Model 3 and Model 4, respectively. (b) The dynamics of population obtained from the studied models. (c) The RMSD errors obtained from Model 4 when the initial time for the FDE model is varying between 216 to 230. (d) The dark blue region is the dynamic behavior of Model 4, when only the order derivative of variable E is changed after Day 280, $0.4 \leq \alpha_E \leq 0.98$, and the blue line is the dynamics with integer orders (Model 2). (e) Heatmap of log_{10} of the errors, RMSD, achieved from Model 3 and (f) Model 4, when only one order derivative is a non-integer value from the interval (0.6,1). Here, orange indicates a worse fit, light blue shows a similar fit, and dark blue implies a better fit than Model 2 with integer orders. (For interpretation of the references to color in this figure legend, the reader is referred to the web version of this article.)

higher value, when there is a worse fit than one obtained from Model 2 with integer orders, while dark blue shows a better fit and light blue implies a similar fit. Hence, this figure suggests that changing only one derivative order throughout the whole time could not achieve a better fit than the model with integer orders. Nevertheless, considering fractional orders in the middle time interval (e.g. day 280 in Model 4) can make a more accurate simulation, see Fig. 1 (e). The dynamics of the selected rectangle of this heatmap, when the order derivative of E is changing, is shown in Fig. 1 (d).

5.1. Numerical methods and implementation

We have implemented all numerical results in Julia. For solving FDE model (8), we utilized the FdeSolver.jl package (v1.0.7), which

is encoded based on product-integration rules and predictor–corrector algorithms [20]. To estimate the values of the parameters, we have used Turing.jl [21] for applying Bayesian inference and Hamiltonian Monte Carlo (HMC) and DifferentialEquations.jl [22] for solving the ODE model (1). We considered the normal distribution $\mathcal{N}(0.1, 0.9)$ for β_r bounded to the intervals $(0.1, 0.9)$, and $\mu \propto \mathcal{N}(0, 0.1)$ bounded to the intervals $(0, 0.1)$. For the parameters α_2 and μ_2, we set a distribution of $\mathcal{N}(0, .0001)$ bounded to the interval $(0, 0.0001)$. For optimizing the order of derivatives, we have used FdeSolver.jl with the function (L)BFGS from the Optim.jl package [23], which are based on the (Limited-memory) Broyden–Fletcher–Goldfarb–Shanno algorithm.

6. Conclusion

We have introduced a novel 8-dimensional nonlinear differential equation model for the Ebola virus disease that includes a dynamic population to simulate its transmission dynamics. We have analyzed the basic reproduction number of the model and have shown that the disease-free equilibrium is locally asymptotically stable when the basic reproduction number is less than one.

To fit real data of the Ebola epidemic in Guinea, Liberia, and Sierra Leone obtained from WHO, we have integrated fractional derivatives into the model. Our numerical analysis has compared four different models, including (1) an ODE model with a constant population, (2) an ODE model with a variable population, (3) an FDE model with a variable population and incommensurate fractional orders from the initial time, and (4) a piecewise differential equation model which starts with the ODE Model 2 and continues with the FDE Model 3. Our results reveal that the last model offers the best fit to the data as measured by root mean square deviation, and outperforms other models we considered.

CRediT authorship contribution statement

Faïçal Ndaïrou: Conceptualization, Data curation, Formal analysis, Funding acquisition, Investigation, Methodology, Project administration, Resources, Software, Supervision, Validation, Visualization, Writing – original draft, Writing – review & editing. **Moein Khalighi:** Conceptualization, Data curation, Formal analysis, Funding acquisition, Investigation, Methodology, Project administration, Resources, Software, Supervision, Validation, Visualization, Writing – original draft, Writing – review & editing. **Leo Lahti:** Conceptualization, Data curation, Formal analysis, Funding acquisition, Investigation, Methodology, Project administration, Resources, Software, Supervision, Validation, Visualization, Writing – original draft, Writing – review & editing.

Declaration of competing interest

The authors declare that they have no known competing financial interests or personal relationships that could have appeared to influence the work reported in this paper.

Data availability

Data available in Github(DOI: https://doi.org/10.5281/zenodo.7646063).

Acknowledgments

This study has been supported by the Academy of Finland, Finland (330887 to MK, LL) and the UTUGS graduate school of the University of Turku, Finland (to MK). The work of Ndaïrou has been partially supported by the Portuguese Foundation for Science and Technology (FCT) within project UIDB/04106/2020 (CIDMA). Ndaïrou is also grateful to the support of FCT, Portugal through the Ph.D. fellowship PD/BD/150273/2019. The authors wish to acknowledge CSC-IT Center for Science, Finland, for computational resources and high-speed networking.

References

[1] Area I, Losada J, Ndaïrou F, Nieto JJ, Tcheutia DD. Mathematical modeling of 2014 Ebola outbreak. Math Methods Appl Sci 2017;40(17):6114–22.
[2] Area I, Ndaïrou F, Nieto JJ, Silva CJ, Torres DFM. Ebola model and optimal control with vaccination constraints. J Ind Manag Optim 2018;14(2):427–46.
[3] Hincapié-Palacio D, Ospina J, Torres DFM. Approximated analytical solution to an Ebola optimal control problem. Int J Comput Methods Eng Sci Mech 2016;17(5–6):382–90.
[4] Rachah A, Torres DFM. Dynamics and optimal control of Ebola transmission. Math Comput Sci 2016;10:331–42.
[5] Siettos C, Anastassopoulou C, Russo L, Grigoras C, Mylonakis E. Modeling the 2014 Ebola virus epidemic-agent-based simulations, temporal analysis and future predictions for Liberia and Sierra Leone. PLOS Curr Outbreaks 2015 March 9, edition 1 2015.
[6] Webb G, Browne C, Huo X, Seydi O, Seydi M, Magal P. A model of the 2014 Ebola epidemic in West Africa with contact tracing. PLoS Curr 2015.
[7] Astacio J, Briere DM, Guillén M, Martínez J, Rodríguez F. and others. Mathematical models to study the outbreaks of Ebola. MTBI technical report, 1996, https://mtbi.asu.edu/research/archive/paper/mathematical-models-study-outbreaks-ebola.
[8] Lekone PE, Finkenstädt BF. Statistical inference in a stochastic epidemic SEIR model with control intervention: Ebola as a case study. Biometrics 2006;62(4):1170–7+1287–1288.
[9] Ndanguza D, Tchuenche JM, Haario H. Statistical data analysis of the 1995 Ebola outbreak in the democratic Republic of Congo. Afr Mat 2013;24(1):55–68.
[10] Area I, Batarfi H, Losada J, Nieto JJ, Shammakh Á. On a fractional order Ebola epidemic model. Adv Difference Equ 2015;2015:278, 12 pp.
[11] Gire SK, Goba A, Andersen KG, et al. Genomic surveillance elucidates Ebola virus origin and transmission during the 2014 outbreak. Science 2014;345(6202):1369.
[12] WHO Ebola Response Team. Ebola virus disease in West Africa — The first 9 months of the epidemic and forward projections. New Engl J Med 2014;371(16):1481–95.
[13] Gantmacher FR. The theory of matrices, vols. 1 and 2. Providence, RI: MS Chelsea Publishing; 1998.
[14] Liénard A, Chipart H. Sur le signe de la partie réelle des racines d'une équation algébrique. J Math 1914;10(6):291–346.
[15] Diekmann O, Heesterbeek JAP, Metz JAJ. On the definition and the computation of the basic reproduction ratio R 0 in models for infectious diseases in heterogeneous populations. J Math Biol 1990;28:365–82.
[16] Du M, Wang Z, Hu H. Measuring memory with the order of fractional derivative. Sci Rep 2013;3:3431.
[17] Saeedian M, et al. Memory effects on epidemic evolution: The susceptible-infected-recovered epidemic model. Phys Rev E 2017;95(2):022409, 9.
[18] Kilbas AA, Srivastava HM, Trujillo JJ. Theory and applications of fractional differential equations. North-Holland Mathematics Studies, vol. 204, Science B.V. Amsterdam: Elsevier; 2006.
[19] Podlubny I. Fractional differential equations. Mathematics in science and engineering, vol. 198, San Diego, CA: Academic Press Inc.; 1999.
[20] Khalighi Moein, Benedetti Giulio, Lahti Leo. Fdesolver: A julia package for solving fractional differential equations. 2022, arXiv:2212.12550.
[21] Ge Hong, Xu Kai, Ghahramani Zoubin. Turing: A language for flexible probabilistic inference. In: Storkey Amos, Perez-Cruz Fernando, editors. Proceedings of the twenty-first international conference on artificial intelligence and statistics. volume 84 of proceedings of machine learning research, PMLR; 2018, p. 1682–90, 09–11.
[22] Rackauckas Christopher, Nie Qing. Differentialequations. jl–A performant and feature-rich ecosystem for solving differential equations in Julia. J Open Res Softw 2017;5(1).
[23] Patrick KM, et al. JuliaNLSolvers/Optim.jl: release 1.7.3. 2022, Zenodo.